Journal of Multidisciplinary Engineering Science and Technology (JMEST)
ISSN: 3159-0040
Vol. 2 Issue 9, September - 2015

Strategy for Design of a Robust Controller for Linear Control Systems

Prof. Kamen M. Yanev
Professor, Department of Electrical Engineering, Faculty of Engineering and Technology
University of Botswana
Gaborone, Botswana
yanevkm@yahoo.com; yanevkm@mopipi.ub.bw

***Abstract*—The contribution of this paper is in suggesting a useful technique for design of a robust controller. The approach to the controller design is compensation with two degrees of freedom, enforcing desired system performance. The design steps are demonstrated for linear, control systems with variable parameters. The controller will restrain the effects of parameters variations. The robust controller improves the quality of the system's performance in terms of its stability, transient response, and sensitivity.**

Keywords—robust; controller; design steps; dominant poles; stability; transient responses, sensitivity, compensation;

I. INTRODUCTION

A useful technique is proposed to design a high quality universal robust controller for linear control systems. A number of design steps introduce a proper multi-stage compensation. The suggested method of the controller design is introducing compensation with two degrees of freedom that put into effect the desired system performance. The robust compensator is connected in series with the original control system and introduces specifically designed new dominant poles. This improves the quality of the system's performance in terms of its stability, transient response and sensitivity in case of variation of the system's parameters.

Control systems usually require performance criteria that consider simultaneously the response error *e(t)* and the time *t* at which it occurs. A very useful criterion is the Integral of Time multiplied by the Absolute value of Error (ITAE) [1].

Considering a second order system, ITAE has a minimum if the damping ratio is $\zeta = 0.707$. This value will be taken as a performance objective targeted by the proposed optimization design. If a system is higher than the second order, a pair of dominant poles can represent the system dynamics. Then, ζ can still be used to indicate the location of these poles and the damping ratio is referred as the relative damping ratio of the system.

When designing the robust controller, to meet the ITAE criterion the following system objectives are set:

Damping ratio $\zeta = 0.707$
Percent Maximum Overshoot (PMO) $\leq$ 4%
Settling-to-Maximum overshoot time $t_s/t_m \leq 1.4$
Steady-State error $e_{ss} \leq 1\%$ (type 0 systems)

These objectives will be used for establishing the design steps and applying the suggested method.

II. DESIGN OF THE ROBUST CONTROLLER STAGES

As an example for a design of a robust controller, a solar-tracker control system is considered [2]. The open-loop transfer function of the system is reflected as the plant transfer function G_{P1} (s) and is presented as:

$$G_{P1}(s) = \frac{K}{s(1+Ts)(1+0.005s)} = \frac{K}{0.005Ts^3 + (T+0.005)s^2 + s} \tag{1}$$

It is assumed that the system has two variable parameters which are the system's gain *K* and one of the system's time-constants *T*. Initially, the time-constant is set to *T* = 0.02 sec, while *K* is let to be the variable. The robust controller consists of two stages: a series stage G_{S1}(s) and a forward stage G_{F1}(s). They are incorporated in the control system as shown in Figure 1.

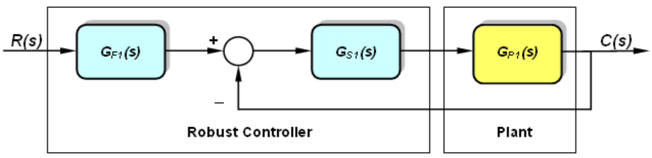

Fig. 1: Two-Step Robust Controller Incorporated in the Control System

The following design steps are considered:

Step 1: The robust controller is going to be built on basis of the desired performance of the plant's closed-loop system. Then, initially the plant G_{P1} *(s)* as a stand-alone block, is involved in a unity feedback system. Its closed-loop transfer function $G_{CL1}(s)$ at *T* = 0.02 sec is presented as:

$$G_{CL1}(s) = \frac{K}{s(1+Ts)(1+0{,}005s)+K} = \frac{K}{0.0001s^3 + 0.025s^2 + s + K} \tag{2}$$

Step 2: The strategy for constructing the series stage $G_{S1}(s)$ of the controller is to place its two zeros near the desired dominant closed-loop poles that satisfy the ITAE criterion. The reason for this is that after applying the unity negative feedback to the cascade connection of $G_{S1}(s)$ and $G_{P1}(s)$, these zeros will appear as dominant poles of the closed-loop system involving the plant and the series controller stage. In order to determine the optimal desired dominant closed-loop poles, it is important to establish the optimal value of the gain K corresponding to ζ = 0,707. This is established by plotting the relationship $\zeta = f(K)$ with the aid of the following code:

```
>>K=[15:0.01:25];
>> for n=1:length(K)
   G_array(:,:,n)=tf([10000*K(n)],[1  250  10000 10000*K(n)]);
   end
>> [y,z]=damp(G_array);
>> plot(K,z(1,:))
```

The optimal value of the gain that corresponds to relative damping ratio ζ = 0,707 is K = 19.82. It is determined with the aid of interactive MATLAB procedure, based on the plot $\zeta = f(K)$, as shown in Figure 2.

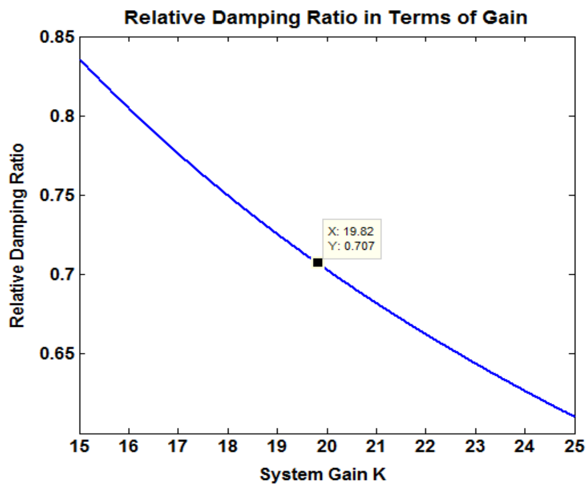

Figure 2: Gain K = 19.82 Corresponding to Damping ζ = 0,707

Step 3: If the optimal gain value K = 19.82 is substituted in equation (4.4), the transfer function of the closed-loop system is modified to:

$$G_{CL1}(s) = \frac{198200}{s^3 + 250s^2 + 10000s + 198200} \tag{3}$$

To determine the desired closed-loop poles, corresponding to the optimal gain value K = 19.82, the following procedure is performed:

```
>> GCL1=tf([198200],[1 250 10000 198000])
>> damp(GCLo)
   Eigenvalue              Damping      Freq. (rad/s)

-2.19e+001 + 2.19e+001i   7.07e-001    3.10e+001
-2.19e+001 - 2.19e+001i   7.07e-001    3.10e+001
-2.06e+002                1.00e+000    2.06e+002
```

It is seen from the code that the desired closed-loop poles are −21.9 ± j21.9.

Step 4: The desired closed-loop poles can be approximated to −22 ± j22 and are placed as zeros to the series controller stage $G_{S1}(s)$. These zeros will appear as dominant poles of the closed-loop system involving the plant and the series stage $G_{S1}(s)$.The transfer function of the series robust controller $G_{S1}(s)$ is presented as:

$$G_{S1}(s) = \frac{(s+22+j22)(s+22-j22)}{968} = \frac{s^2+44s+968}{968} \tag{4}$$

Step 5: To realize physically the $G_{S1}(s)$, two remote poles at $s_{1,2}$ = (−1250, j0) can be added with negligible effect on the system performance.

To simplify the analysis, the transfer function of the cascade connection of the series controller stage and the plant will still be determined by implementing the equation (4) as follows:

$$\begin{aligned} G_{OL1}(s) &= G_{S1}(s)G_{P1}(s) = \\ &= \frac{0.001K(s^2+44s+968)}{0.005Ts^3+(T+0.005)s^2+s} = \\ &= \frac{0.001K(s^2+44s+968)}{0.0001s^3+0.025s^2+s} \end{aligned} \tag{5}$$

Step 6: When G_{OL1}(s) is involved in a unity feedback system, its closed-loop transfer function is determined as:

$$G_{CL1S}(s) = \frac{0.001K(s^2+44s+968)}{\left[\begin{array}{l} 0.0001s^3+0.025s^2+s+ \\ +0.001K(s^2+44s+968) \end{array}\right]} \tag{6}$$

Step 7: As seen from the equation (6), the closed-loop zeros will attempt to cancel the closed loop poles of the system, being in their vicinity.

To avoid this problem, a forward controller G_{F1}(s) is added in cascade to the closed-loop system G_{CL1S}, with the purpose to cancel the zeros of G_{CL1S}. Therefore, the transfer function of the forward controller is selected as follows:

$$G_{F1}(s) = \frac{968}{s^2+44s+968} \tag{7}$$

Step 8: By combining all the cascade stages, the transfer function of the total compensated system is determined as:

$$G_{T1}(s) = G_{F1}(s)G_{CL1S}(s) =$$

$$= \frac{K}{0.0001s^3 + 0.025s^2 + s + 0.001K(s^2 + 44s + 968)} \quad (8)$$

III. D-Partitioning Analysis of the Robust Control System

To compare the system margin of stability before and after the robust compensation, the D-Partitioning analysis [3], [4] can be applied in terms of the variable parameter *K.*

The characteristic equation of the original closed-loop system is determined as:

$$G(s) = s(1+0.02s)(1+0.005s) + K = 0 \quad (9)$$

Then, the variable parameter *K* can be obtained as follows:

$$K(s) = -\frac{P(s)}{Q(s)} = -\frac{s(1+0.02s)(1+0.005s)}{1} = -\frac{0.0001s^3 + 0.025s^2 + s}{1} \quad (10)$$

The D-partitioning in terms of the variable parameter *K*, as seen from Figure 3, is obtained with the aid of the MATLAB code as shown below, considering $s = j\omega$ and varying the frequency within the range $-\infty \le \omega \le +\infty$.

The D-partitioning curve can be plotted in the complex plane facilitated by MATLAB the “nyquist” m-code.

```
>> K=tf([0.0001 0.025 1 0],[0 1])
Transfer function:
 -0.0001 s^3 - 0.025 s^2 – s
>>nyquist(K)
```

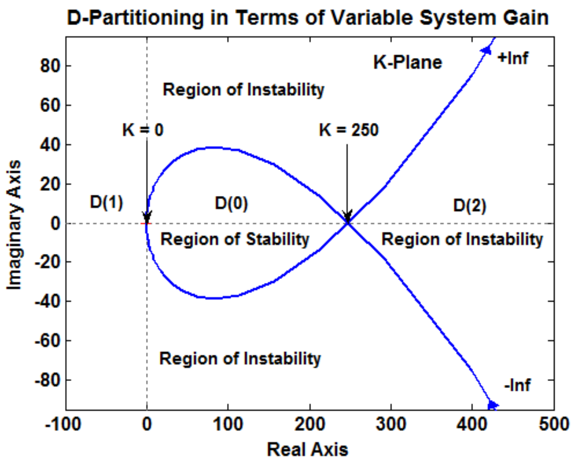

*Fig. 3: D-Partitioning in Terms of the Gain K **before** the Robust Compensation*

The D-partitioning determines three regions on the *K*-plane: D(0), D(1) and D(2). Only D(0) is the region of stability, being the one, always on the left-hand side of the curve for a frequency variation from $-\infty$ to $+\infty$. The system is stable within the range of the servo amplifier gain $0 \le K \le 250$ that can be proven in a similar way like for the systems of Type 0.

After the compensation, the variable parameter *K* can be determined from the characteristic equation of (8) as follows:

$$K = -\frac{0.0001s^3 + 0.025s^2 + s}{0.001s^2 + 0.044s + 1} \quad (11)$$

The D-Partitioning curve after the application of the robust compensation is plotted with aid of the code:

```
>> K = tf([-0.0001 -0.025 -1 0],[0.001 0.044 2])
Transfer function:
-0.0001 s^3 - 0.025 s^2 - s
---------------------------
 0.001 s^2 + 0.044 s + 2
>> nyquist(K)
```

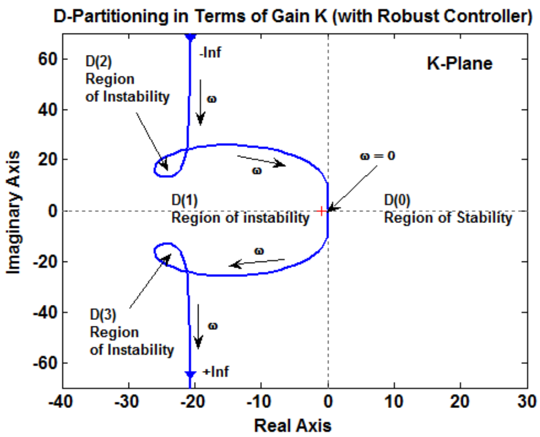

Fig. 4: *D-Partitioning in Terms of the Gain K **after** the Robust Compensation*

The D-Partitioning determines four regions of the *K*-plane: D(0), D(1), D(2) and D(3). As seen from Figure 4, Only D(0) is the region of stability, being always on the left-hand side of the D-Partitioning curve for a frequency variation from $-\infty$ to $+\infty$.

By comparing Figure 3 and Figure 4, it is seen that the robust controller has improved considerably the margin of stability of the compensated system. While the original system becomes marginal at $K = 250$, after the robust compensation, the system will be stable for any positive values of the gain, or $K > 0$.

IV. Transient Response Analysis of the Robust Control System

Consideration of the system’s transient responses is used for the analysis and comparison of the system robustness before and after the compensation [3], [4]. The system’s transient responses before the robust compensation for different values of the gain within the region of the system's stability, K = 20, 50 and 100, are determined considering the transfer function of the original plant (1), where the time constant is set to T = 0.02 sec. The following code is applied:

```
>> Gp120=tf([0 20],[0.0001 0.025 1 0])
>> Gp150=tf([0 50],[0.0001 0.025 1 0])
>> Gp1100=tf([0 100],[0.0001 0.025 1 0])
>> Gp1fb20=feedback(Gp120,1)
>> Gp1fb50=feedback(Gp150,1)
>> Gp1fb100=feedback(Gp1100,1)
>> step(Gp1fb20,Gp1fb50,Gp1fb100)
```

The compensated system is examined for robustness considering the system's transient responses, by substituting random even higher values for the system's gain, K = 100, K = 200, K = 500, in the equation of the transfer function (8), corresponding to the compensated robust system:

$$G_{T1}(s)_{K=100} = \frac{100}{0.0001s^3 + 0.125s^2 + 5.4s + 96.8} \quad (12)$$

$$G_{T1}(s)_{K=200} = \frac{200}{0.0001s^3 + 0.225s^2 + 9.8s + 193.6} \quad (13)$$

$$G_{T1}(s)_{K=500} = \frac{500}{0.0001s^3 + 0.525s^2 + 23s + 484} \quad (14)$$

The transient responses of the system for the three different cases of the gain variation are determined by the code:

```
>> GT100 = tf([100], [0.0001 0.125 5.4 96.8])
>> GT200 = tf([200],[0.0001 0.225 9.8 193.6])
>> GT500 = tf([500], [0.0001 0.525 23 484])
>> step(GT100,GT200,GT500)
```

Taking into account the codes shown above, the system's transient responses achieved before and after the robust compensation are reflected accordingly in Figure 5 and 6.

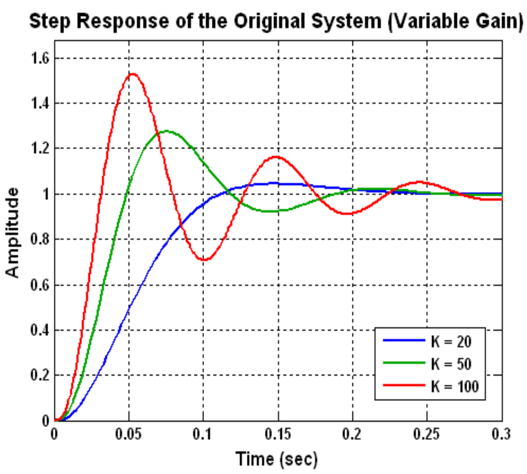

*Fig. 5: Transient Responses of the Original Control System **before** the Robust Compensation (K = 20, K = 50, K = 100)*

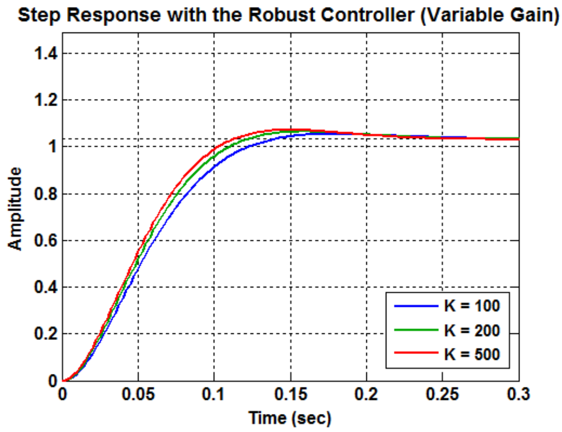

*Fig. 6: Transient Responses of the Robust Control System **after** the Robust Compensation (K = 100, K = 200, K = 500)*

As seen from Figure 6, due to the effect of the applied robust controller, the system becomes quite insensitive to considerable variation of the gain K. Experiments of the robust system with gain variation within the limits $0.5K < K < 5K$ prove that the system is quite insensitive to variations of the gain K.

Since the considered system is with two variable parameters, now the time-constant is altered, as follows: T = 0.001 sec, T = 0.02 sec, T = 0.08 sec, while keeping the system's gain at K = 200. Initially these values are substituted in equation (1) that is the transfer function of the original system as follows:

```
>> Gp1001=tf([0 200],[0.000005 0.006 1 0])
>> Gp102=tf([0 200],[0.0001 0.025 1 0])
>> Gp108=tf([0 200],[0.0004 0.085 1 0])
>> Gp1fb001=feedback(Gp1001,1)
>> Gp1fb02=feedback(Gp102,1)
>> Gp1fb08=feedback(Gp108,1)
>> step(Gp1fb001,Gp1fb02,Gp1fb08)
```

Further, the values T = 0.001 sec, T = 0.02 sec, T = 0.08 sec and K = 100 are substituted in equation (8) of the robust compensated system:

$$G_{T1}(s)_{T=0.001} = \frac{200}{0.000005s^3 + 0.306s^2 + 14.2s + 193.6} \quad (15)$$

$$G_{T1}(s)_{T=0.02} = \frac{200}{0.0001s^3 + 0.325s^2 + 14.2s + 193.6} \quad (16)$$

$$G_{T1}(s)_{T=0.08} = \frac{200}{0.0004s^3 + 0.385s^2 + 14.2s + 193.6} \quad (17)$$

The transient responses of the compensated robust control system of Type 1 for the three different cases representing the time constant variation are determined by the code:

```
>> GT0001 = tf([200],[0.000005 0.306 14.2 193.6])
>> GT002 = tf([200], [0.0001 0.325 14.2 193.6])
>> GT008 = tf([200],[0.0004 0.385 14.2 193.6])
>> step(GT0001,GT002,GT008)
```

The comparison of the system robustness before and after the compensation is reflected in Figure 7 and Figure 8:

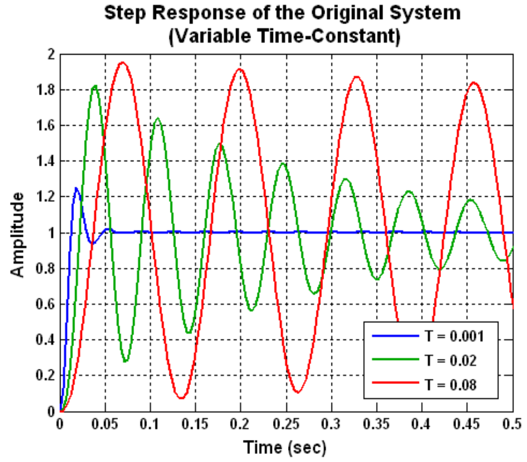

Fig. 7: Step Responses of the Original System ***before*** *the Robust Compensation*
(T = 0.001 sec, T = 0.02 sec, T = 0.08 sec at K = 200)

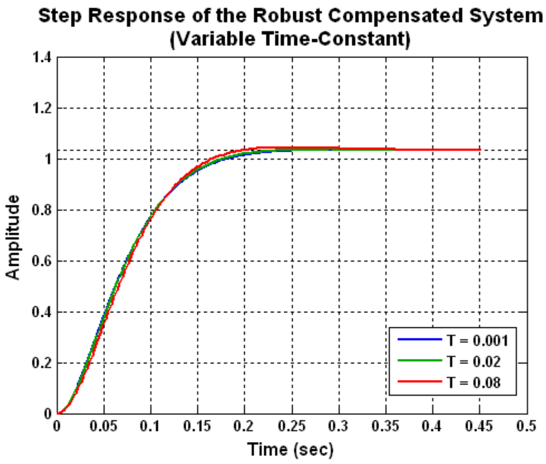

Fig. 8: *Transient Responses of the System* ***after*** *the Robust Compensation*
(T = 0.001 sec, T = 0.02 sec, T = 0.08 sec at K = 200)

As seen from Figure 8, the compensated robust control system is quite insensitive to considerable variation of the time constant *T*. Experiments after the application of the robust controller with the time constant variation within the limits $0.1T < T < 10T$, demonstrate that the system is still quite insensitive to variations of the time constant. To assess the system's performance after the application of the robust controller, an average system case is chosen with K = 300 and T = 0.02 sec. This case will differ insignificantly from the other cases of the discussed variable K and T. The performance evaluation is accomplished by the following code:

```
>> GT002 = tf([300],[0.0001 0.325 14.2 290.4])
>> damp(GT002)
  Eigenvalue                  Damping     Freq. (rad/s)
 -2.20e+001 + 2.05e+001i      7.31e-001    3.01e+001
 -2.20e+001 - 2.05e+001i      7.31e-001    3.01e+001
 -3.21e+003                   1.00e+000    3.21e+003
```

It is seen from the results that the system's relative damping ratio is ζ = 0.731, being insignificantly different from the objective ζ = 0.707.

The system's Percentage Maximum Overshoot (PMO) is determined by substituting the determined value of the relative damping ratio ζ = 0.731 in the following equation:

$$PMO = 100e^{-\pi\varsigma/\sqrt{1-\varsigma^2}} = 3.47\% \tag{18}$$

The system's settling time (t_S) is defined as the time required for the step response to be brought within a specified percentage of its final value. For a specified limit of ±5% t_S is determined by substituting the obtained values of the relative damping ratio ζ = 0.731 and the natural frequency ω_n = 30.1 rad/sec as follows:

$$t_{S(5\%)} = \frac{4.6}{\varsigma\omega_n} = 0.209 \text{ sec} \tag{19}$$

The system's time to maximum overshoot and the time ratio are determined similarly as follows:

$$t_m = \frac{\pi}{\omega_n\sqrt{1-\varsigma^2}} = 0.153 \text{ sec} \tag{20}$$

$$t_{S(5\%)} / t_m = 1.366 \tag{21}$$

As seen from Table I, all the achieved results are meeting the ITAE criterion, since they have values that match or are lower than the targeted objectives.

TABLE I COMPARISON BETWEEN THE OBJECTIVES AND THE REAL RESULTS

Specifications	Objectives	Real Results	Consideration
ζ	= 0.707	= 0.731	Close Match
PMO	≤ 4%	= 3.47%	Better
$t_{s(5\%)}/t_m$	≤ 2.5	= 1.366	Better

The performance evaluation results of t_S and t_m are also confirmed by the system step response determined in the time domain.

V. Robust System Sensitivity in Case of Parameter Uncertainties

The sensitivity interpretation [5], [6] of a system with respect to parameter variations can be easily achieved with the aid of the frequency-domain plots. A comparison between the sensitivity of the original and the compensated systems confirm the obtained results established in the time-domain. Taking into account an original control systems of with a unity feedback, its general transfer function is:

$$W(s) = \frac{G_P(s)}{1 + G_P(s)} \tag{22}$$

If taking into consideration the variations of any of the parameters of the original open-loop system, represented by the plant transfer function $G_P(s)$, the sensitivity of $W(s)$ with respect to any variations of $G_P(s)$ is determined as follows [6], [7]:

$$S_G^W(s)=\frac{dW(s)/W(s)}{dG_p(s)/G_p(s)}=\frac{G_p(s)^{-1}}{1+G_p(s)^{-1}}=\frac{1}{1+G_p(s)} \qquad (23)$$

The best sensitivity value is considered $S_G^W(s)=0$.

Taking into account the system with the transfer function described by equation (1) and substituting it into equation (23) for T = 0.02 sec and the cases K = 100, K = 200 and K = 500, the sensitivities of the original system are:

$$S^W_{G1\,OriginalK=100}(s)=\frac{0.0001s^3+0.025s^2+s}{0.0001s^3+0.025s^2+s+100} \qquad (24)$$

$$S^W_{G1\,OriginalK=200}(s)=\frac{0.0001s^3+0.025s^2+s}{0.0001s^3+0.025s^2+s+200} \qquad (25)$$

$$S^W_{G1\,OriginalK=500}(s)=\frac{0.0001s^3+0.025s^2+s}{0.0001s^3+0.025s^2+s+500} \qquad (26)$$

Similarly, taking into account the total robust control system described by equation (8) and substituting it in (23), the sensitivities are determined as:

$$S^{WR}_{GT1\,RobustK=100}(s)=\frac{0.0001s^3+0.125s^2+5.4s+96.8}{0.0001s^3+0.125s^2+5.4s+196.8} \qquad (27)$$

$$S^{WR}_{GT1\,RobustK=200}(s)=\frac{0.0001s^3+0.225s^2+9.8s+193.6}{0.0001s^3+0.225s^2+9.8s+393.6} \qquad (28)$$

$$S^{WR}_{GT1\,RobustK=500}(s)=\frac{0.0001s^3+0.525s^2+23s+484}{0.0001s^3+0.525s^2+23s+984} \qquad (29)$$

The sensitivity functions (24), (25), (26) and (27), (28), (29) are plotted in the frequency domain with the aid of the following code and shown in Figure 9.

```
>> G1OriginalK100=tf([0.0001 0.025 1 0],[0.0001 0.025 1 100])
>> G1OriginalK200=tf([0.0001 0.025 1 0],[0.0001 0.025 1 200])
>> G1OriginalK500=tf([0.0001 0.025 1 0],[0.0001 0.025 1 500])
>> G1RobustK100=tf([0.0001 0.125 5.4 96.8],[0.0001 0.125 5.4 196.8])
>> G1RobustK200=tf([0.0001 0.225 9.8 193.6],[ 0.0001 0.225 9.8 393.6])
>> G1RobustK500=tf([0.0001 0.525 23 484],[ 0.0001 0.525 23 984])
>>bode(G1OriginalK100,G1OriginalK200,G1OriginalK500,G1RobustK100,G1RobustK200,G1RobustK200)
```

As seen from Figure 9, the sensitivity of the original control systems are $S_G^W(s)\geq 0\text{dB}$ in the frequency range 65 rad/sec < ω < 400 rad/sec, reaching $S_G^W(s)=21.6\text{dB}$ for the case of K = 200. The sensitivity of the robust system for the case of K = 100, coincide with the cases of K = 200 and K = 500.

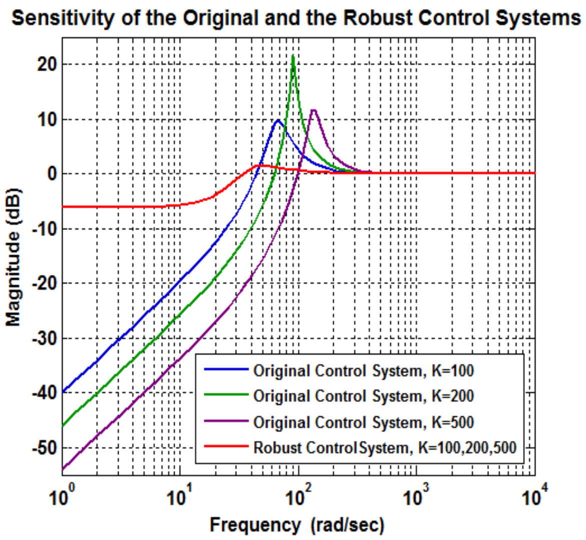

Fig. 9: Sensitivity of the Original Type 1 System and the Robust Control System (Variable Gain K)

From Figure 9 is seen that the robust system is again with considerably lower sensitivity compared with the original one.

Considering the same system and substituting equation (1) into (23) for K = 300 and the cases T = 0.001 sec, T = 0.02 sec and T = 0.08 sec, the sensitivities of the original system are:

$$S^W_{G1\,OriginalT=0.001}(s)=\frac{0.000005s^3+0.006s^2+s}{0.000005s^3+0.006s^2+s+300} \qquad (30)$$

$$S^W_{G1\,OriginalT=0.02}(s)=\frac{0.0001s^3+0.025s^2+s}{0.0001s^3+0.025s^2+s+300} \qquad (31)$$

$$S^W_{G1\,OriginalT=0.08}(s)=\frac{0.0004s^3+0.085s^2+s}{0.0004s^3+0.085s^2+s+300} \qquad (32)$$

Taking into consideration the total robust control system described by equation (8) and substituting it in (23), the sensitivities are determined as:

$$S^{WR}_{GT1\,RobustT=0.001}(s)=\frac{0.000005s^3+0.306s^2+14.2s+290.4}{0.000005s^3+0.306s^2+14.2s+590.4} \qquad (33)$$

$$S^{WR}_{GT1\,RobustT=0.02}(s)=\frac{0.0001s^3+0.325s^2+14.2s+290.4}{0.0001s^3+0.325s^2+14.2s+590.4} \qquad (34)$$

$$S^{WR}_{GT1\,RobustT=0.08}(s)=\frac{0.0004s^3+0.385s^2+14.2s+290.4}{0.0004s^3+0.385s^2+14.2s+590.4} \qquad (35)$$

The sensitivity functions derived from the original system and described by the equations (30), (31), (32) and those derived from the robust system and described by equations (33), (34), (35) are plotted in the frequency domain as shown in Figure 10 with the aid of the following code:

```
>> G1OriginalT0001=tf([0.000005 0.006 1 0],[0.000005 0.006 1 300])
>> G1OriginalT002=tf([0.0001 0.025 1 0],[0.0001 0.025 1 300])
>> G1OriginalT008=tf([0.0004 0.085 1 0],[0.0004 0.085 1 300])
>> G1RobustT0001=tf([0.000005 0.306 14.2 290.4],[0.000005 0.306 14.2 590.4])
>> G1RobustT002=tf([0.0001 0.325 14.2 290.4],[0.0001 0.325 14.2 590.4])
>> G1RobustT008=tf([0.0004 0.385 14.2 290.4],[0.0004 0.385 14.2 590.4])
>>bode(G1OriginalT0001,G1OriginalT002,G1OriginalT008,
        G1RobustT0001,G1RobustT002,G1RobustT008)
```

From Figure 10 is seen that the robust system is with significantly lower sensitivity compared with the one of the original system, again proving the improved robustness of the system after the compensation.

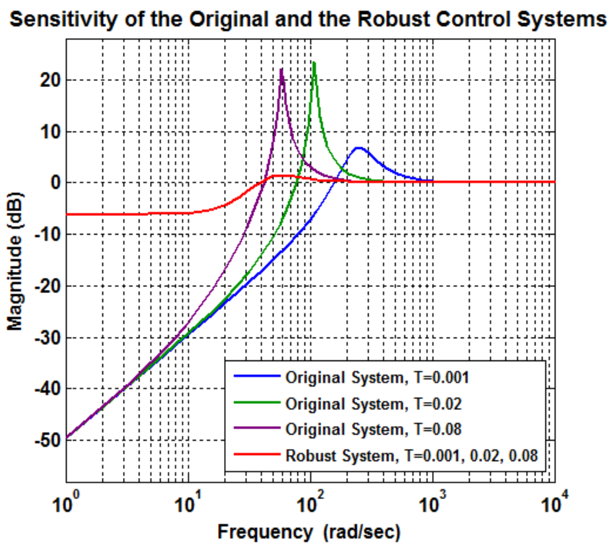

Fig. 10: Sensitivity of the Original Type 1 System and the Robust Control System (Variable Time-Constant T)

VI. ROBUST SYSTEM SENSITIVITY IN CASE OF DISTURBANCE AND NOISE

In many control system applications, the system must yield performance that is robust not only to parameter variations, but also to external disturbances and noise. Although, feedback employing high loop gain in conventional control systems has the ability of reducing the effects of external disturbances and noise, robustness achieved in this way is detrimental to stability. Alternatively, the required robust effect can be accomplished by applying the designed in this research controller.

If the noise is $N(s) = 0$, the disturbance-to-output transfer function is presented as follows [6], [7]:

$$Q_{Robust\,D}(s) = \frac{C(s)}{D(s)} = \frac{1}{1+G_S(s)G_P(s)} \tag{36}$$

The best case of disturbance rejection would be if $Q_{Robust\,D}(s) = 0$ [6], [7].

If the disturbance is $D(s) = 0$, the noise-to-output transfer function is:

$$Q_{Robust\,N}(s) = \frac{C(s)}{N(s)} = -\frac{G_S(s)G_P(s)}{1+G_S(s)G_P(s)} \tag{37}$$

Considering the original system, described by equation (1) and the robust system, described by equations (8) and also taking into consideration equations (36), the disturbance-to-output transfer function for the original and the robust control systems are represented as follows:

$$Q_{Original\,D1}(s) = \frac{0.0001s^3+0.025s^2+s}{0.0001s^3+0.025s^2+s+200} \tag{38}$$

$$Q_{Robust\,D1}(s) = \frac{0.0001s^3+0.025s^2+s}{0.0001s^3+0.2316s^2+10.1s+200} \tag{39}$$

Again, the true improvement of the disturbance rejection is analyzed by comparing the transfer functions $Q_{OriginalD1}(s)$ and $Q_{RobustD1}(s)$ in the frequency domain. The functions (4.75) and (4.76) are plotted as Bode magnitudes in the frequency domain with the aid of the following code and shown in Figure 4.26.

```
>> Q1OriginalK200=tf([0.0001 0.025 1 0],[0.0001 0.025 1 200])
>> Q1RobustK200=tf([0.0001 0.025 1 0],[0.0001 0.231 10.1 200])
>>bode(Q1OriginalK200,Q1RobustK200)
```

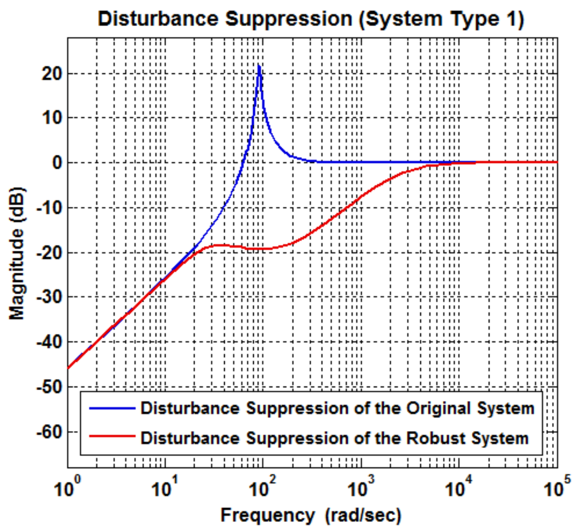

Fig. 11: Disturbance Rejection of the Original Control System Type 1 and the Robust Control System

Figure 11 reveals that the disturbance rejection of the original control system is $Q_{OriginalD1} \geq 0$ dB in the frequency range 60 rad/sec $< \omega <$ 300 rad/sec, reaching $Q_{OriginalD1}$ = 21.6 dB at 90.6 rad/sec. By applying the robust controller, the disturbance rejection is significant. The magnitude Bode plot of disturbance-to-output function is $Q_{RobustD1} \leq 0$ in the full frequency range.

The noise-to-output transfer functions for the original and the robust control systems are represented as follows:

$$Q_{OriginalN1}(s) = -\frac{300}{0.0001s^3 + 0.025s^2 + s + 300} \quad (40)$$

$$Q_{RobustN1}(s) = -\frac{0.031s^2 + 13.64s + 300}{0.0001s^3 + 0.3356s^2 + 14.64s + 300} \quad (41)$$

The functions (4.79) and (4.80) are plotted in the frequency domain, as shown in Figure 4.28, with the aid of the following code:

```
>> Q1OriginalK300N=tf([-300],[0.0001 0.025 1 300])
>> Q1RobustK300N=tf([-0.031 -13.64 -300],[0.0001 0.335 14.64 300])
>> bode(Q1OriginalK300N,Q1RobustK300N)
```

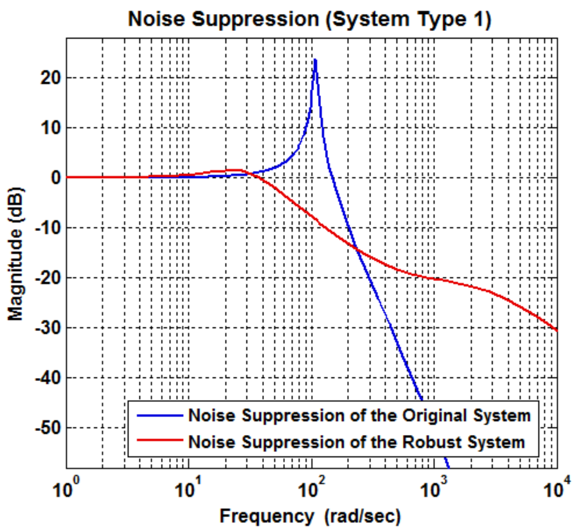

Fig. 12: *Noise Suppression of the Original Control System Type 1 and the Robust Control System*

The actual improvement of the noise rejection is analyzed by comparing the transfer functions $Q_{OriginalN1}(s)$ and $Q_{RobustN1}(s)$ in the frequency domain. As seen from Figure 12, after applying the robust controller, the noise rejection is significant, again proving the efficiency of the robust controller in terms of Noise rejection as well.

VII. Conclusions

The design strategy of a robust controller for linear control systems proves that by choosing and implementing desired dominant system poles, the controller enforces the required relative damping ratio and system performance.

The robust controller has an effect of bringing the system to a state of insensitivity to the variation of its parameters within specific limits of the parameter variations. The experiments in the time-domain with variation of different parameters show only insignificant difference in performance for the different system conditions.

Since the design of the robust controller is based on the desired system performance in terms of relative damping, its contribution and its unique property is that it can operate effectively for any of the system's parameter variations or simultaneous variation of a number of parameters. This property is demonstrated by the comparison of the system's performance before and after the application of the robust controller. Tests demonstrate that the system performance in terms of damping, stability and time response remains robust and insensitive in case of any simultaneous variations of the gain and the time-constant within specific limits.

The results from the sensitivity analysis illustrate that the introduction of the designed robust controller considerably reduces the system's sensitivity to multivariable parameter uncertainties and therefore improves the robustness of the system.

From the results, it is also seen that the robust controller has the effect of considerable suppression of the disturbance and noise, bringing their additive components to the system's output signal close to zero.

References

[1] Shinners J. S., Modern Control System Theory, 3rd ed., New York: McGraw-Hill, pp.190-203, 2004.

[2] Yanev K.M., Masupe S., Robust design and efficiency in case of parameters uncertainties, disturbances and noise, International Review of Automatic Control, Vol. 5, N. 6, ISSN: 1974-6059, pp. 860-867, 2012.

[3] Yanev, K.M., Anderson G.O., Masupe S., D-partitioning analysis and design of a robust photovoltaic light tracker system, BIE 12th Annual Conference, 6001, ISBN: 97899912-0-731-5, 2011.

[4] Neimark Y.,D-partition and robust stability, Computational Mathematics and Modeling, 9(2), pp. 160-166, 2006.

[5] Kuo B.C., Automatic control systems, New York, USA, McGraw-Hill, pp.521-530, 2010.

[6] Yanev K.M., Analysis of systems with variable parameters and robust controller design, Proceedings of the Sixth IASTED International Conference on Modeling, Simulation and Optimization, MSO 2006, Gaborone, Botswana, p. 75-83, 2006.

[7] Yanev K.M, Anderson G.O, Masupe S., Multivariable system's parameters interaction and robust control design, Journal of International Review of Automatic Control, Vol. 4, N.2 pp.180-190, 2011.